Research Article

Corni Fructus Alleviates UUO-Induced Renal Fibrosis via TGF-*β*/Smad Signaling

Jin A. Lee ⓘ **, Mi-Rae Shin** ⓘ **, and Seong-Soo Roh** ⓘ

Department of Herbology, College of Korean Medicine, Daegu Haany University, 136, Sinchendong–ro, Suseong-gu, Daegu 42158, Republic of Korea

Correspondence should be addressed to Seong-Soo Roh; ddede@dhu.ac.kr

Renal fibrosis is a type of chronic kidney disease (CKD) induced by infiltration of inflammatory cells, myofibroblast accumulation, and ECM production in the kidney. From a long time ago, Corni Fructus (CF) is known to supplement the liver and kidney with its tepid properties. In this study, we investigated the renal protective mechanism of CF, which is known to supplement the kidney, in rat model of unilateral ureteral obstruction (UUO). After inducing UUO through surgery, the group was separated ($n = 8$) and the drug was administered for 2 weeks; normal rats (normal), water-treated UUO rats (control), CF 100 mg/kg-treated UUO rats (CF100), and CF 200 mg/kg-treated UUO rats (CF200). As a result of histopathological examination of kidney tissue with H&E, MT, and PAS staining, it was confirmed that the infiltration of inflammatory cells and the erosion of collagen were relatively decreased in the kidneys treated with CF. Also, CF significantly reduced the levels of MDA and BUN in serum. As a result of confirming the expression of the factors through western blotting, CF treatment significantly reduced the expression of NADPH oxidase and significantly regulated the AMPK/LKB1/NF-*κ*B pathway associated with inflammation. In addition, it downregulated the expression of major fibrotic signaling factors, such as *α*-SMA, collagen I, MMP-2, and TIMP-1, and significantly regulated the TGF-*β*1/Smad pathway, which is known as a major regulator of renal fibrosis. Taken together, these findings indicate that CF can alleviate renal fibrosis by regulating the TGF-*β*1/Smad pathway through inhibition of oxidative stress in UUO.

1. Background

Chronic kidney disease (CKD) is a disease that refers to when symptoms, such as abnormal kidney function and structure, decrease in function persist for more than 3 months and is recognized as a major health problem due to high medical costs and mortality [1, 2]. CKD is caused by obesity, smoking, and continuous exposure to nephrotoxic drugs and causes complications such as cardiovascular disease, diabetes, dyslipidemia, and bone and mineral disorders [2, 3]. Also, various chronic kidney diseases, such as ureteral obstruction and diabetes, can cause inflammatory cell infiltration and myofibroblast accumulation, and it induces excessive accumulation of extracellular matrix (ECM) through induction of increased ECM production and decreased degradation, leading to renal fibrosis [4, 5]. Inflammation and oxidative stress play an important role

in the cause of renal fibrosis. Several studies have shown that oxidative stress is involved in the activation of transforming growth factor *β*1 (TGF-*β*1) activity, a major pathway for fibrosis [6, 7]. TGF-*β*1 signals are transmitted to the intermediate Smad, and especially, Smad2 and Smad3 are considered as major pathogenic mechanism of renal fibrosis [8]. Currently, several studies aimed at inhibiting TGF-*β*1 signaling have shown good results for the treatment of renal fibrosis, but limited advances have been made in translating this research to patients with CKD [9].

In traditional Korea medicine (TKM), Corni Fructus (CF) is the dry ripe sarcocarp of *Cornus officinalis* Siet. et Zucc., which is classified into the family of Cornaceae, commonly known as dogwoods. In TKM theory, CF has sour and astringent and is known to supplement the liver and kidney with its tepid properties [10]. In line with the theory of supplying the liver and kidneys, various studies have

shown that CF improves liver damage in acute alcoholic liver injury and alleviates kidney damage in diabetes [11]. In addition, various pharmacological effects of CF such as reduction of oxidative stress, anti-inflammatory, and cancer cell apoptosis are known [12–15]. As active constituents of CF, loganin, morroniside, gallic acid, sweroside, cornin, etc. are known [16]. Gallic acid is a polyphenol-based compound and is well known for its high antioxidant activity; for loganin and morroniside, studies on the renal protective effect in diabetes are being actively conducted [17–21]. In addition, various effects such as apoptosis and alleviation of inflammation through the NF-κB pathway are known [22, 23].

In this study, renal inflammation and fibrosis were induced through unilateral ureteral obstruction (UUO), and the renal protective effect of CF in renal fibrosis was evaluated. To elucidate the underlying mechanism of CF, which is known to supplement the kidney and inhibition of oxidative stress, we examined the NADPH oxidase and TGF-β1/Smad pathways in renal fibrosis.

2. Materials and Methods

2.1. Materials. 2-thiobarbituric acid, phenyl methane sulfonyl fluoride (PMSF), and 1,1,3,3-tetramethoxypropane were purchased from Sigma-Aldrich (St, Louis, MO, USA). Phosphoric acid was purchased from Duksan company (Ansan, Korea). The protease inhibitor mixture solution was purchased from Wako Pure Chemical Industries, Ltd. (Osaka, Japan). The pierce BCA protein assay kit was purchased from Thermo Fisher Scientific (Waltham, MA, USA). ECL western blotting detection reagents and pure nitrocellulose membranes were purchased from GE Healthcare (Chicago, IL, USA). NOX2 (SC-130543), p22^{phox} (SC-271968), Rac1 (SC-217), LKB1 (SC-32245), p-LKB1 (SC-271924), IκBα (SC-1643), p-IκBα (SC-8404), NF-κBp65 (SC-8008), TGF-β1 (SC-130348), Smad2/3 (SC-8332), p-Smad2/3 (SC-11769), Smad4 (SC-7966), Smad7 (SC-365846), MMP-2 (SC-13595), TIMP-1 (SC-21734), β-actin (SC-47778), and histone (SC-8030) were used antibodies of Santa Cruz Biotechnology, Inc. (Dallas, TX, USA). AMPK (#2532) and p-AMPK (#2531) were used antibodies of Cell Signaling Technology, Inc. (Danvers, MA, USA). α-SMA (ab5694) and collagen I (ab34710) were used antibodies of Abcam (Cambridge, England). Goat anti-rabbit and goat anti-mouse immunoglobulin G (IgG) horseradish peroxidase- (HRP-) conjugated secondary antibodies were purchased from GeneTex, Inc. (Irvine, CA, USA). Zoletil®50 was purchased from Virbac Laboratory (Carros, France), and Isotroy was purchased from Troikaa Pharmaceuticals, Ltd. (Ahmedabad, India).

2.2. Preparation of the Plant Material. Corni Fructus (CF) was purchased from Omniherb Co., Ltd. (Daegu, Korea). A voucher herbarium specimen was verified at the College of Korean Medicine in Daegu Haany University. The herb dried Corni Fructus (100 g) was extracted by 10 times of distilled water (100°C) during 2 h. The solvent was concentrated in evaporated *in vacuo* and dried completely using a freeze dryer to obtain a powder (the yield rate of CF; 25.7%).

2.3. CF Analysis by HPLC Chromatogram. Each sample (10 mg) was dissolved in 10 mL of 50% methanol and filtered through a Dismic-13 JP membrane filter. We injected 20 μL of the sample into a reverse-phase HPLC using a Phenomex Gemini NX C18 (4.6 × 150 mm, 3 μm pore size), with a column temperature of 35°C. Mobile phase component was as follows: solvent A (0.1% formic acid) and solvent B (acetonitrile). The gradient conditions are as follows: A : B = 100 : 0 (0 min) $\longrightarrow$ 100 : 0 (3 min) $\longrightarrow$ 90 : 10 (5 min) $\longrightarrow$ 90 : 10 (7 min) $\longrightarrow$ 80 : 20 (12 min) $\longrightarrow$ 70 : 30 (17 min) $\longrightarrow$ 70 : 30 (22 min) $\longrightarrow$ 40 : 60 (31 min) $\longrightarrow$ 40 : 60 (35 min) $\longrightarrow$ 5 : 95 (40 min) $\longrightarrow$ 5 : 95 (43 min) $\longrightarrow$ 50 : 50 (45 min). The flow rate was 0.6 mL/min. The UV absorbance from 277 nm was monitored using an Agilent 1200 series with a multiwavelength detector (Agilent Technologies, San Jose, CA, USA). All peaks were assigned by carrying out coinjection tests with authentic samples and comparing them with the UV spectral data. The measurement was repeated three times for each sample. Representative HPLC results are illustrated in Figure 1. Quantification of gallic acid, morroniside, and loganin in the extract was performed by peak area measurement (gallic acid, 27 mg/g; morroniside, 361 mg/g; loganin, 514 mg/g).

2.4. Unilateral Ureteral Obstruction (UUO) Model. The animal experiments were performed according to the "Guidelines for Animal Experiment" approved by Ethics Committee of the Daegu Haany University (Approval no. DHU2021-047). The 7-week-old male Sprague-Dawley rats (body weight, 200~240 g) were purchased from DaehanBio-Link (Eumseong, Korea) and used for the experiments after being adapted to environment for 1 week. Environmental conditions were set to 12 h light/dark cycle, controlled humidity (50 ± 5%), and temperature (22 ± 2°C). After 1 week adaptation, the rats were randomly divided into 4 groups (n = 8/group) as follows: the normal group (normal), the UUO+distilled water treatment group (control), the UUO+100 mg/kg/day CF treatment group (CF100), and the UUO+200 mg/kg/day CF treatment group (CF200). Rats were given intraperitoneal anesthesia with tiletamine and zolazepam (Zoletil®50; 37.5 mg/kg). The left ureter was isolated through a median incision and was ligated at 2 points with 2–0 silk. From the day after the operation, the drug corresponding to the each group was orally administered for 2 weeks, and on the 15th day after the operation, animals were euthanized and the kidneys were collected. Kidneys were immediately stored at -80°C.

2.5. Histological Examination. The kidneys were stained with three of the most suitable dyes, such as hematoxylin & eosin (H&E), Masson's trichrome (MT), and periodic acid-Schiff (PAS). The kidneys were fixed in 10% buffered formalin and then embedded in paraffin. These were sectioned with 3 μm thickness (H&E) and 5 μm thickness (MT and PAS). PAS-stained sections (0.5% periodic acid; 10 min, Schiff solution; 10 min) were counterstained with Harris hematoxylin for 3 min (at 25°C) and differentiated in 1% HCl-EtOH mixture, followed by blue color development in 0.5% ammonia water (30 s), dehydration in ethanol, cleaning in xylene,
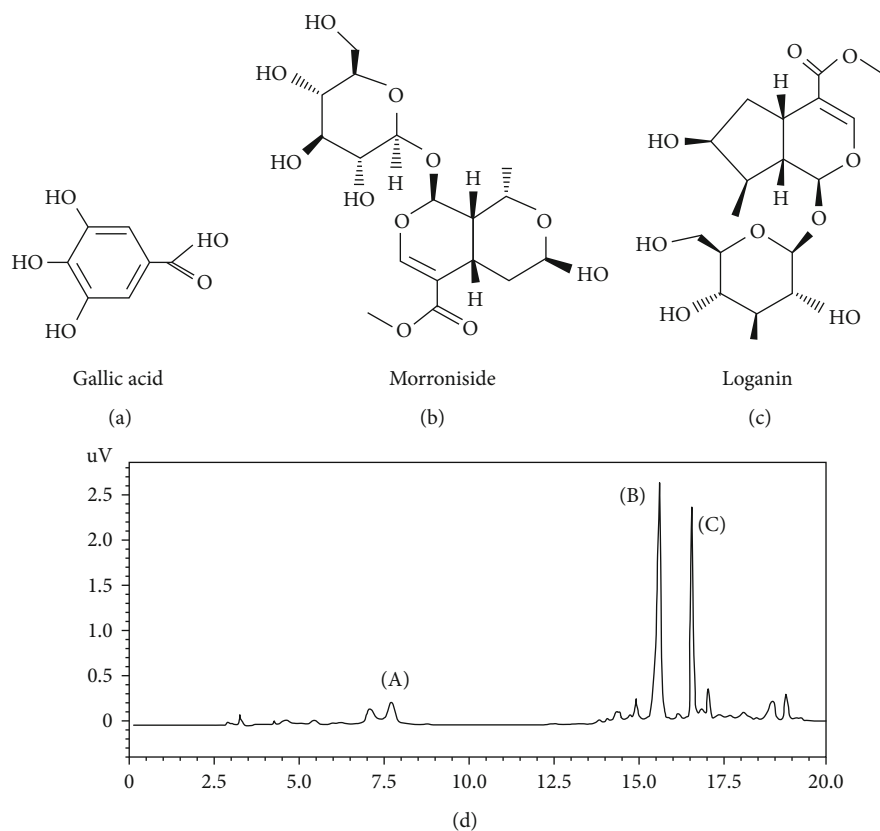
FIGURE 1: Analysis of gallic acid, morroniside, and loganin in the extract of CF. (a) Chemical structure of gallic acid. (b) Chemical structure of morroniside. (c) Loganin. (d) HPLC chromatogram of the extract of CF.

and examination. Each slide was observed and analyzed using the i-Solution Lite (IMT i-Solution Inc., Burnaby, BC, Canada). Quantification analysis of each positive signal for histological examination image was obtained from the randomly selected sections of at least 3 fields of each sample using Image J 1.8.0 software (U.S. National Institutes of Health, Bethesda, MD, USA).

2.6. Measurement of MDA Level. The malondialdehyde (MDA) level was measured according to the method of Mihara and Uchiyama [24]. 1,1,3,3,-tetramethoxypropane was used as a standard sample. After mixing sample and 1% phosphoric acid, 0.67% thiobarbituric acid was added, and boiling for 45 min at 95°C. After that, mixed butanol, and centrifuge (3,000 rpm, 10 min) to use supernatant. Dispense the supernatant, and absorbance was measured at 540 nm using a UV-VIS spectrophotometer.

2.7. Measurement of BUN Level. The blood urea nitrogen (BUN) level was measured using specific assay kit and a microplate fluorescence reader (Asan, Seoul, Korea).

2.8. Preparation of Nuclear and Cytosol Factions. The extraction of protein was performed as described by Komatsu [25]. For cytosol fractions, kidney tissues were homogenized with lysis buffer A containing 10 mM HEPES (pH 7.8), 10 mM KCl, 2 mM $MgCl_2$, 1 mM DTT, 0.1 mM EDTA, 0.1 mM PMSF, and protease inhibitor mixture solution. The tissue

homogenates were incubated (4°C for 30 min), and then, 10% NP-40 was mixed well. After centrifugation (12,000 rpm at 4°C for 2 min) using Eppendorf 5415R (Hamburg, Germany), the supernatant (cytosol fractions) was separated to new Eppendorf tubes. The pellets were washed twice by the lysis buffer and discard the supernatant. After that, the pellets were suspended with lysis buffer C containing 300 mM NaCl, 50 mM HEPES (pH 7.8), 50 mM KCl, 1 mM DTT, 0.1 mM PMSF, 0.1 mM EDTA, and 1% (v/v) glycerol, and protease inhibitor mixture solution was suspended and incubated (4°C for 30 min). After centrifugation (12,000 rpm at 4°C for 10 min), the supernatant (nuclear fractions) was collected in new tubes. For the estimation of NOX2/p22^{phox}/Rac1/p-AMPK/AMPK/p-LKB1/LKB1/p-IκBα/IκBα/NF-κBp65/α-SMA/collagen I/MMP-2/TIMP-1/p-Smad2/3/Smad2/3/Smad4/Smad7/□-actin/histone, 12 μg of proteins was electrophoresed through 8-12% sodium dodecyl sulfate polyacrylamide gel (SDS-PAGE). Separated proteins were transferred to a nitrocellulose membrane, blocked with 5% (w/v) skim milk solution for 1 h, then incubated with primary antibodies (1 : 1000), respectively, overnight at 4°C. After the blots were washed, they were incubated with anti-rabbit or anti-mouse IgG HRP-conjugated secondary antibody (1 : 3000) for 2 h at room temperature. Each antigen-antibody complex was visualized using ECL western blotting detection reagents and detected by chemiluminescence with Sensi-Q 2000 Chemidoc (Lugen Sci Co., Ltd., Gyeonggi-do, Korea). Band densities were measured using ATTO Densitograph
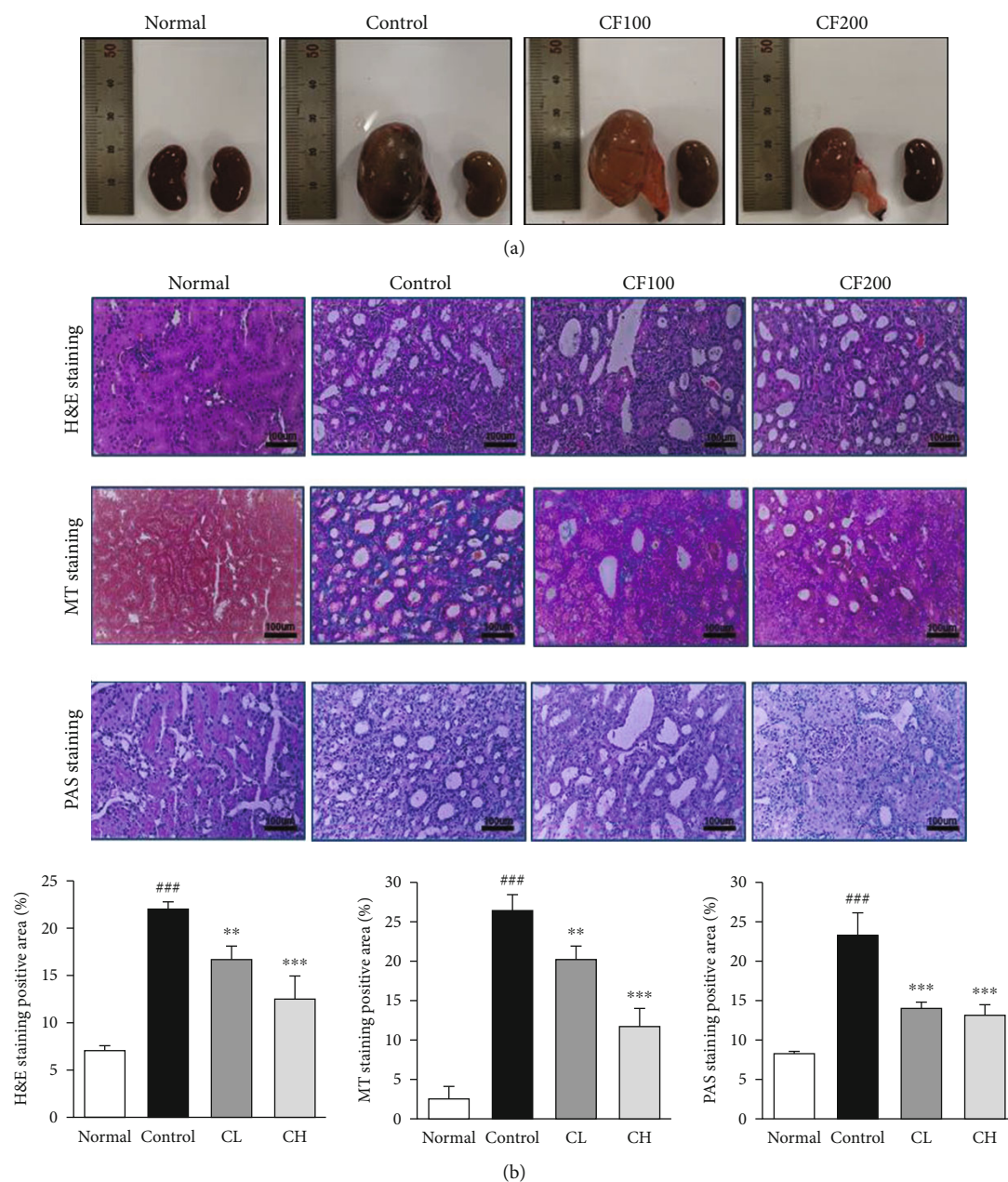
(a)

(b)

Figure 2: Surgical induction of unilateral ureteral obstruction and kidney histological examination. (a) Representative gross image. (b) Kidney histological examination. The scale bars represent $100\,\mu$m (magnification, $\times 200$). H&E staining; the kidneys were stained with Hematoxylin and Eosin; MT staining; the kidney were stained with Masson's trichrome; PAS staining; the kidney were stained with periodic acid-Schiff. Significance: $^{###}P < 0.001$ vs. the normal group and $^{**}P < 0.01$, $^{***}P < 0.001$ vs. the UUO control group.

Software (ATTO Corporation, Tokyo, Japan) and quantified as the ratio to histone or □-actin. The protein levels of the groups are expressed relative to those of the normal rat (represented as 1). We followed the methods of Lee et al. [26].

2.9. Statistical Analysis. Data are presented as the mean ± standard deviation. Statistical comparisons were analyzed by one-way ANOVA tests followed by the least significant difference (LSD) test using SPSS (version 26.0, IBM, Armonk, NY, USA). Values of $P < 0.05$ were considered significant.

3. Results

3.1. Renal Volume and Renal Histopathology. When the renal volumes of the four groups were compared, it was confirmed that the renal volume increased due to ureter obstruction in the control compared to the normal, and the renal parenchyma became thinner. On the other hand, it was confirmed that the renal volume decreased in the group administered with CF, which means that fibrosis due to obstruction was successfully alleviated (Figure 2(a)).

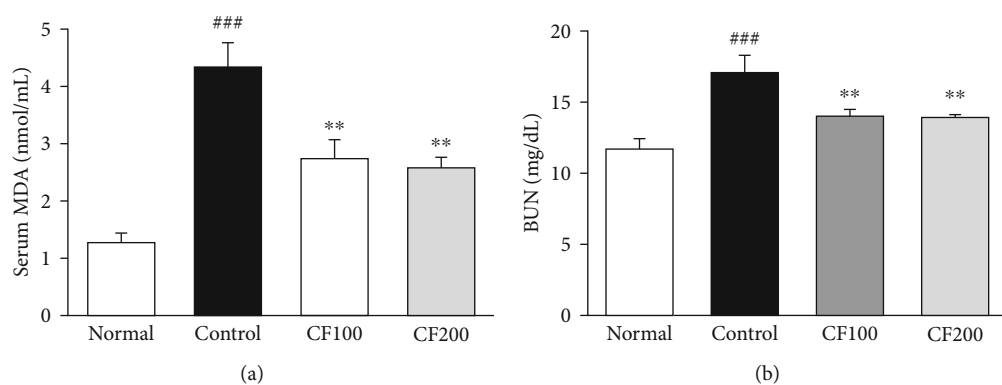To confirm histological changes in the kidney, tissues were examined using H&E, MT, and PAS staining.

FIGURE 3: Effects of CF on MDA and BUN levels. (a) Serum MDA (nmol/mL). (b) Serum BUN (mg/dL). Bar are express as mean ± SD ($n = 8$). Significance: $^{###}P < 0.001$ vs. the normal group and $^{**}P < 0.01$ vs. the UUO control group.
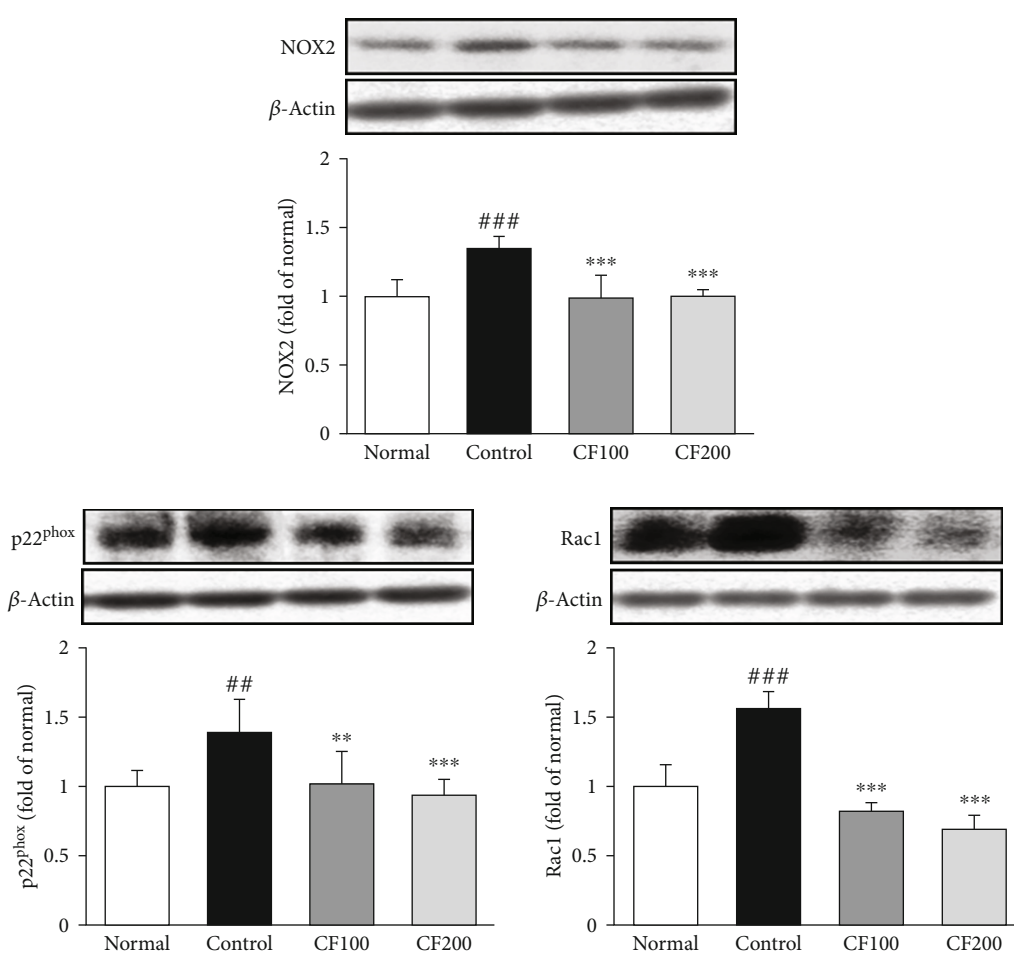

FIGURE 4: Effects of CF on NADPH oxidases. The expressions of NADPH oxidase were measured by western blotting. Bar are express as Mean ± SD (n =8). Significance: $^{##}P < 0.01$, $^{###}P < 0.001$ vs. the normal group and $^{**}P < 0.01$, $^{***}P < 0.001$ vs. the UUO control group.

Representative images are shown in Figure 2(b). In the control compared to normal, it was confirmed that the infiltration of tubular dilatation, inflammatory cells such as neutrophil and the deposition of collagen were increased, and it was confirmed that the infiltration of inflammatory cells and the erosion of collagen were relatively decreased in the kidneys treated with CF.

3.2. Measurement of MDA and BUN Levels. Oxidative stress is known to induce an inflammatory response in the body, and oxidative stress in the kidney causes kidney damage and increases the level of BUN [27]. Figure 3 shows the results of measuring MDA and BUN in serum. MDA level in the control was markedly higher compared with the normal (1.27 ± 0.17 vs.4.34 ± 0.41 mnol/mL, $P < 0.001$). MDA
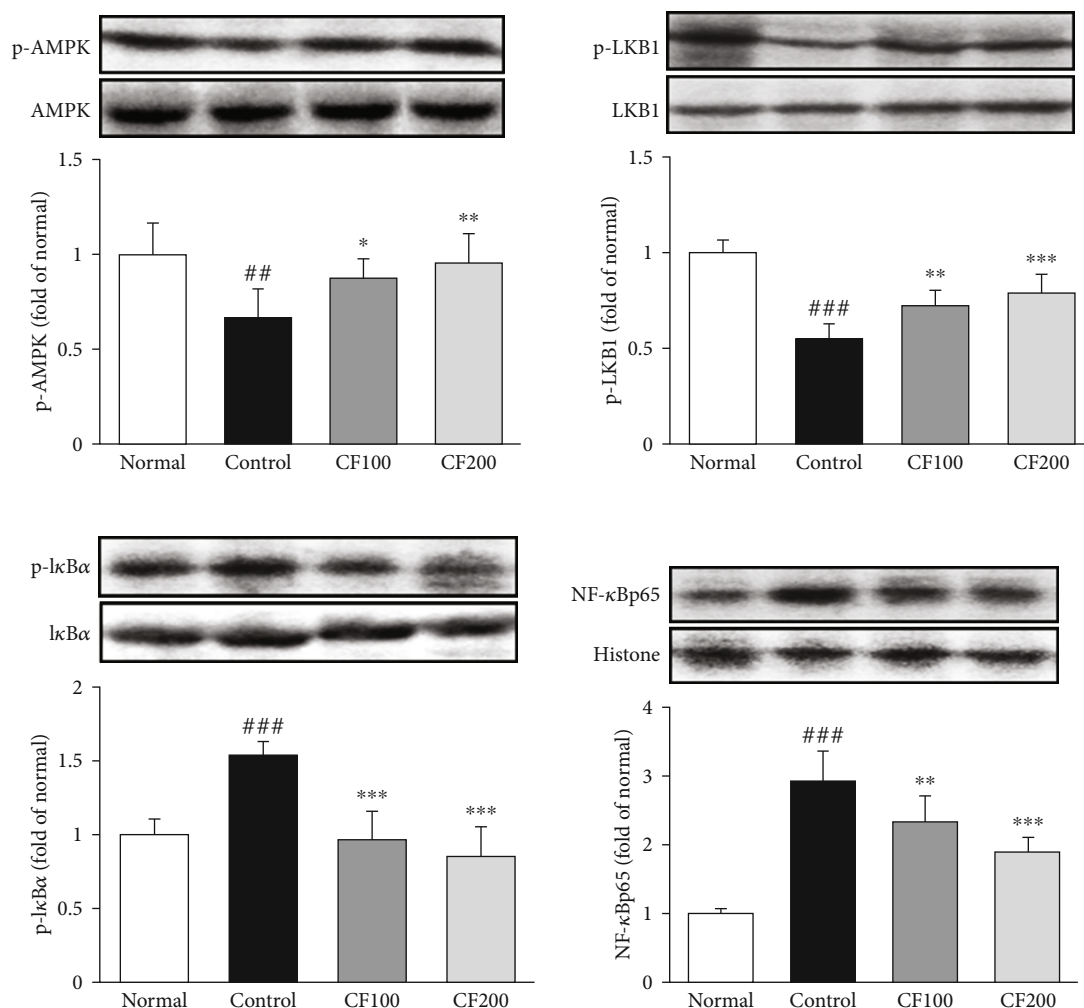
FIGURE 5: Effects of CF on AMPK/LKB1/NF-κB pathway. The expressions of AMPK/LKB1/NF-κB pathway were measured by western blotting. Bar are express as mean ± SD ($n = 8$). Significance: $^{\#\#}P < 0.01$, $^{\#\#\#}P < 0.001$ vs. the normal group and $^{*}P < 0.05$, $^{**}P < 0.01$, $^{***}P < 0.001$ vs. the UUO control group.

levels in CF100 were significantly reduced by 37% compared to the control, and in CF200, MDA level was also significantly reduced by 40%. The level of BUN, which is used as a factor of kidney damage, was also significantly higher in the control than in the normal (11.67 ± 0.66 vs.17.02 ± 1.15 mg/dL, $p < 0.001$), whereas it was confirmed that the CF-treated group significantly decreased compared to the control.

3.3. Expressions of NADPH Oxidase in UUO. A number of previous studies have reported various possible connections between NADPH oxidases and oxidative stress. As shown in Figure 4, NADPH oxidases, including NOX2, p22$^{\text{phox}}$, and Rac1, significantly increased in the UUO control group (NOX2; 1.34 ± 0.09, p22$^{\text{phox}}$; 1.39 ± 0.24, Rac1; 1.56 ± 0.13), whereas CF treatment dramatically decreased such the increase to the level of the normal.

3.4. Response of Inflammation by AMPK/LKB1 and NF-κBp65 Activation in UUO. Expressions of p-AMPK, p-LKB1, p- IκBα, and NF-κBp65 were quantified using western blotting. As shown in Figure 5, CF-treated induced the phos-

phorylation of AMPK and LKB1. The phosphorylation of AMPK and LKB1 reduced the translocation of NF-κBp65 to the nucleus by inhibiting phosphorylation of IκBα.

3.5. Expressions of ECM-Related Protein in UUO. To investigate the effects of CF on remodeling of the ECM, we performed western blot experiments of α-SMA, collagen I, MMP-2, and TIMP-1. Expression of ECM-related proteins is shown in Figure 6. These proteins were expressed at higher levels in the UUO control group than in the normal (α-SMA; 3.30 ± 0.49, collagen I; 1.84 ± 0.13, MMP-2; 1.37 ± 0.19, and TIMP-1; $1.46 \pm .14$). Also, CF-treated group significantly reduced these ECM-related protein levels.

3.6. Expressions of TGF-β1/Smad in UUO. We examined TGF-β1/Smad signaling by means of western blot. As shown in Figure 7, compared with the normal, UUO control group significantly upregulated the protein levels of TGF-β1 and phosphorylated Smad2/3 (TGF-β1; 1.28 ± 0.16 and p-Smad2/3; 1.66 ± 0.17). In addition, in the UUO control group, the expression of Samd4 was significantly upregulated and the
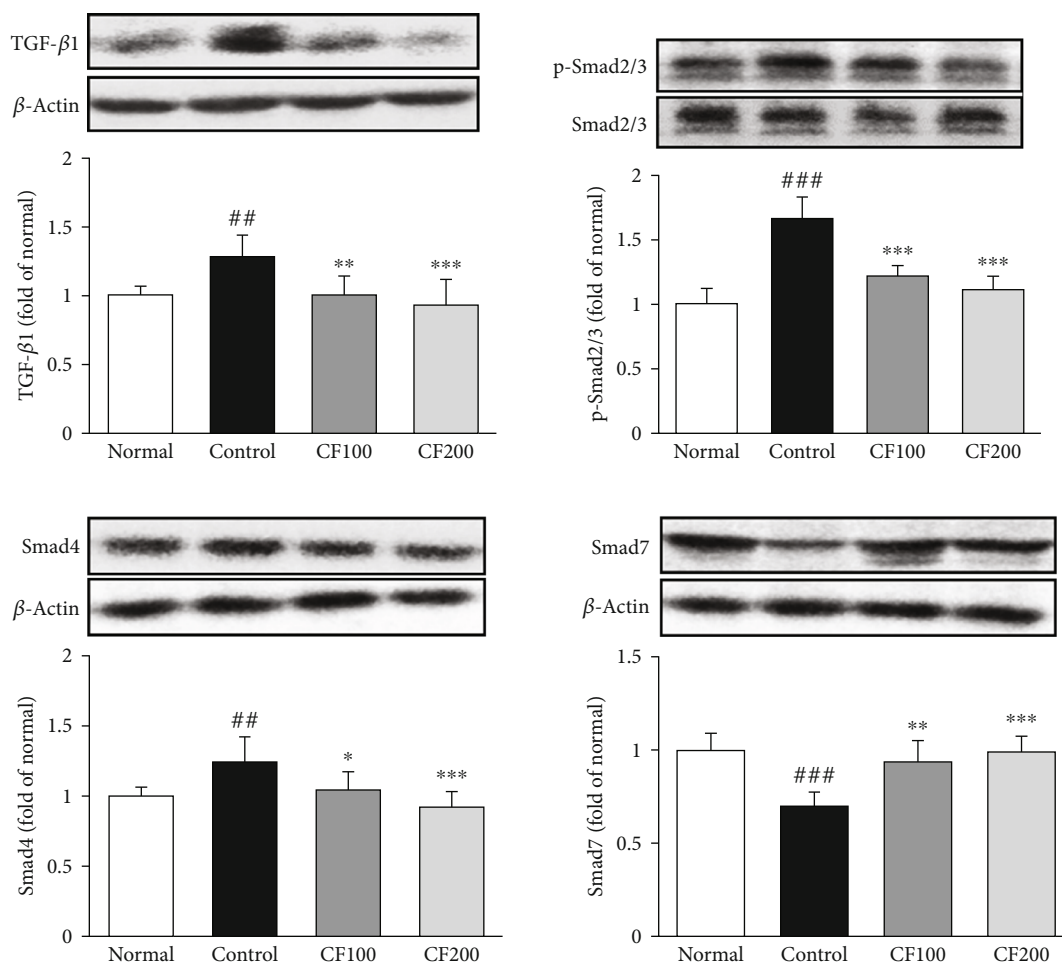
FIGURE 6: Effects of CF on TGF-β1/Smad signaling. The expressions of TGF-β1/Smad signaling were measured by western blotting. Bar are express as mean $\pm$ SD ($n = 8$). Significance: $^{\#\#}P < 0.01$, $^{\#\#\#}P < 0.001$ vs. the normal group and $^{*}P < 0.05$, $^{**}P < 0.01$, $^{***}P < 0.001$ vs. the UUO control group.

expression of Smad7 was downregulated (Smad4; 1.25 ± 0.176 and Smad7; 0.70 ± 0.08). Compared with the UUO control group, the proteins of TGF-β1, p-Smad2/3, Smad4, and Smad7 were all dramatically regulated in the CF-treated group.

4. Discussion

Chronic kidney disease (CKD) is a disease that refers to when symptoms such as abnormal kidney function and structure persist for more than over months; due to its high mortality rate, it is considered a dangerous disease, especially for patients with a history of diabetes, hypertension, and cardiovascular disease [1]. In this study, renal inflammation and fibrosis were induced through unilateral ureteral obstruction (UUO), and the renal protective effect of Corni Fructus (CF) in renal fibrosis was evaluated. CF has been widely used in traditional Korea medicine (TKM) as a supplement for the liver and kidney [11]. In support of this theory, various studies on the renal protective effect of CF have been published [28–30]. In addition, several studies have demonstrated that the active compounds of CF, such as morroniside and logan, have renal protective effects [18, 20]. Active chemical compound of CF was detected by HPLC, and 27 mg/g of gallic

acid, 361 mg/g of morroniside, and 514 mg/g of loganin were detected. These finding showed that CF may play a vital role in the improvement of the kidney. To evaluate the renal protective effect of CF, renal fibrosis was induced in the left kidney of animals. CF improved the increased renal volume and thinned renal parenchyma due to UUO and showed successful remission of fibrosis due to obstruction. Also, it was confirmed that infiltration of lymphocytes and inflammatory cells and deposition of collagen were relatively reduced in the CF-treated group compared to the UUO control group through H&E, MT, and PAS staining.

The kidney is an organ that requires a lot of energy, which makes it more vulnerable to damage caused by oxidative stress (OS) [31]. According to Khan's presentation, OS in chronic kidney disease can promote complications such as hypertension [32], and Manucha Valles reported that oxidative stress directly affects the inflammatory process and apoptosis in obstructive nephropathy [33]. Malondialdehyde (MDA), known as a factor in lipid peroxidation, contributes to OS and is known as one of the most reliable markers for determining oxidative stress [34, 35]. As a result of this experiment, the level of MDA in the serum increased by UUO was significantly reduced in the CF-treated group,
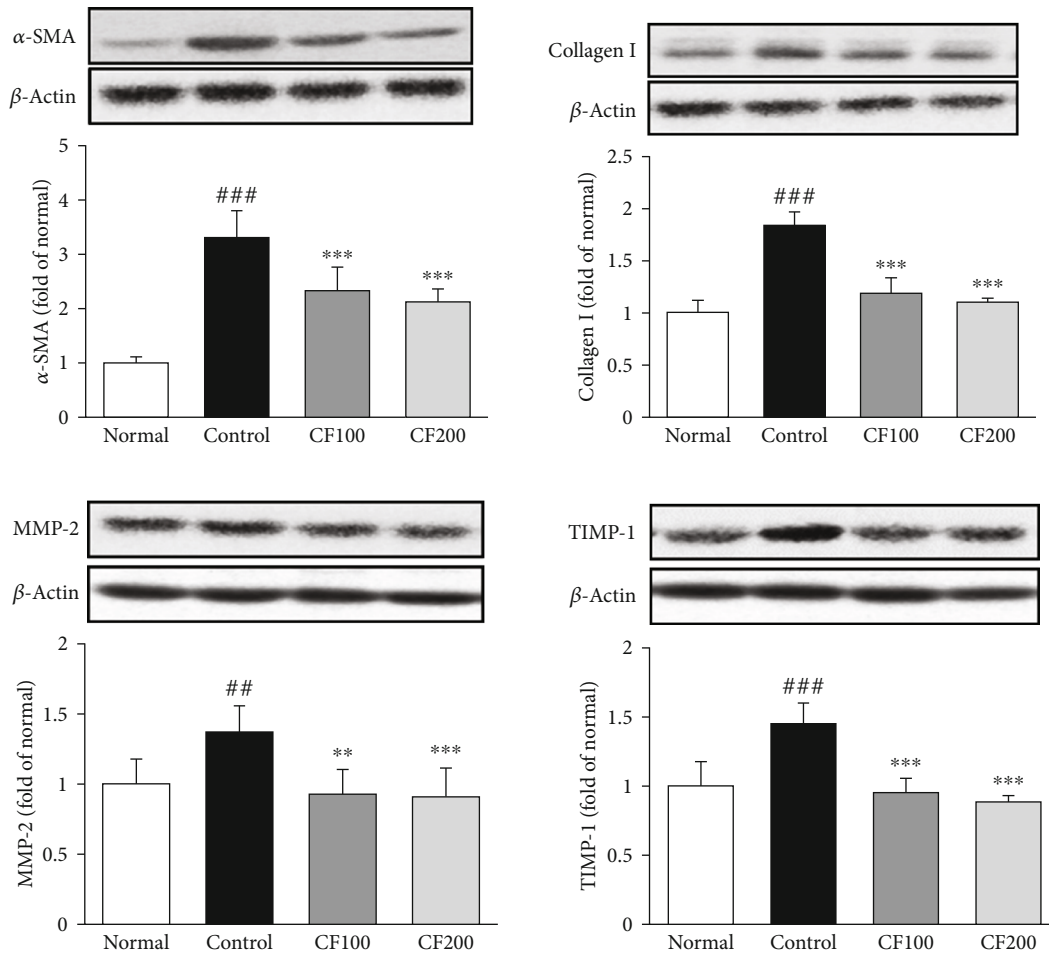
FIGURE 7: Effects of CF on extracellular matrix remodeling. The expressions of extracellular matrix remodeling were measured by western blotting. Bar are express as mean $\pm$ SD ($n = 8$). Significance: $^{##}P < 0.01$, $^{###}P < 0.001$ vs. the normal group and $^{**}P < 0.01$, $^{***}P < 0.001$ vs. the UUO control group.

and the level of BUN, known as a kidney injury biomarker, was also significantly reduced. The other production source about OS is the NADPH oxidase (NOX) family, which has a role in catalyzing the formation of peroxides from oxygen and NADPH [36–38]. Numerous studies have shown that NOX2 is associated with renal fibrosis and can alleviate renal fibrosis by inhibiting NOX2 [39, 40]. As a result of confirming the expression of NOX2, in our study, it was confirmed that the CF-treated group significantly decreased compared to the UUO control group, and the expression of p22^{phox} and Rac1 was also significantly decreased. This is thought to be involved in the alleviation of renal fibrosis in this study as in the previous study that inhibition of NOX2 alleviates renal fibrosis.

AMPK/LKB1 is a pathway that plays a key role in maintaining cellular energy homeostasis. It is known that this pathway promotes the inflammatory response by inducing NF-κB activation and phosphorylation of IκBα. Also, inflammatory response induces the synthesis of fibrosis related factors, leading to renal fibrosis [41–43]. In our study, CF significantly inhibited NF-κB activation via the AMPK/LKB1 pathway, suggesting that CF negatively affects renal fibrosis progression through its anti-inflammatory effect. The extracellular matrix

(ECM) is present in all tissues and regulates various functions such as proliferation, migration, and differentiation of cell. Myofibroblasts induce excessive accumulation of ECM, leading to loss of organ function and fibrosis [44–46]. In this experiment, it was confirmed that the expression of α-SMA and ECM-related factor (collagen I, MMP-2, and TIMP-1) was increased by UUO, and it was confirmed that the down-regulation was confirmed by administration of CF. We investigated TGF-β1/Smad signaling, which is known to be a major regulator of renal fibrosis. Many researchers have demonstrated that TGF-β1 is associated with renal fibrosis. TGF-β1 is induced by fibroblast activation and ECM accumulation and is directly involved in the activation of Smad causing over-expression of fibrosis genes [47, 48]. Receptor-regulated Smads (R-Smad) migrate to the nucleus along with common Smad (co-Smad) to regulate the transcription of genes. In this process, inhibitory Smads (I-Smad) inhibit TGF-β1 signaling, reducing the formation of the R-Smad/co-Smad complex [49]. In this experiment, it was confirmed that the expression of TGF-β1 was suppressed by administration of CF, and the expression of Smad2/3 (R-Smads), Smad4 (co-Smad), and Smad7 (I-Smad) was regulated.

5. Conclusion

Taken together, CF inhibits ECM deposition and TGF-β1/Smad signaling by inhibiting the activity of NF-κB through inhibition of oxidative stress in the UUO. We found that CF impacted renal fibrosis and inflammation in a rat model of UUO. Also, these results suggest that it could be a new material for UUO treatment.

Data Availability

All data are contained within the article.

Conflicts of Interest

The authors declare that they have no competing interests.

Authors' Contributions

JAL wrote the manuscript and carried out the laboratory experiments. MRS carried out the statistical analysis and data analysis. SSR conceived and designed the experiments. All authors read and approved the final manuscript.

Acknowledgments

References

[1] D. Y. Gaitonde, D. L. Cook, and I. M. Rivera, "Chronic kidney disease: detection and Evaluation," *American Family Physician*, vol. 96, no. 12, pp. 776–783, 2017.

[2] G. Eknoyan, N. Lameire, K. Eckardt, and B. Kasiske, "KDIGO 2012 clinical practice guideline for the evaluation and management of chronic kidney disease," *Kidney International. Supplement*, vol. 3, p. 5, 2013.

[3] M. Yang, C. H. Fox, J. Vassalotti, and M. Choi, "Complications of progression of CKD," *Advances in Chronic Kidney Disease*, vol. 18, no. 6, pp. 400–405, 2011.

[4] M. Nishida, Y. Okumura, S. Ozawa, I. Shiraishi, T. Itoi, and K. Hanaoka, "MMP-2 inhibition reduces renal macrophage infiltration with increased fibrosis in UUO," *Biochemical and Biophysical Research Communications*, vol. 354, no. 1, pp. 133–139, 2007.

[5] L. Ling, M. Yang, W. Ding, and Y. Gu, "Ghrelin attenuates UUO-induced renal fibrosis via attenuation of Nlrp3 inflammasome and endoplasmic reticulum stress," *American Journal of Translational Research*, vol. 11, no. 1, pp. 131–141, 2019.

[6] Y. Liu, "Renal fibrosis: new insights into the pathogenesis and therapeutics," *Kidney International*, vol. 69, no. 2, pp. 213–217, 2006.

[7] W. Lv, G. W. Booz, F. Fan, Y. Wang, and R. J. Roman, "Oxidative stress and renal fibrosis: recent insights for the development of novel therapeutic strategies," *Frontiers in Physiology*, vol. 9, p. 105, 2018.

[8] J. Chen and D. Li, "Telbivudine attenuates UUO-induced renal fibrosis via TGF-β/Smad and NF-κB signaling," *International Immunopharmacology*, vol. 55, pp. 1–8, 2018.

[9] S. Y. Lee, S. I. Kim, and M. E. Choi, "Therapeutic targets for treating fibrotic kidney diseases," *Translational Research*, vol. 165, no. 4, pp. 512–530, 2015.

[10] Y. Dong, Z. L. Feng, H. B. Chen, F. S. Wang, and J. H. Lu, "*Corni Fructus*: a review of chemical constituents and pharmacological activities," *Chinese Medicine*, vol. 13, no. 1, p. 34, 2018.

[11] Z. Jiang, J. Wang, H. Xue et al., "Protective effect of wild Corni fructus methanolic extract against acute alcoholic liver injury in mice," *Redox Report*, vol. 22, no. 6, pp. 338–345, 2017.

[12] S. O. Lee, S. Y. Kim, S. M. Han, H. M. Kim, S. S. Ham, and I. J. Kang, "Corni fructus scavenges hydroxy radicals and decreases oxidative stress in endothelial cells," *Journal of Medicinal Food*, vol. 9, no. 4, pp. 594–598, 2006.

[13] Y. H. Sung, H. K. Chang, S. E. Kim et al., "Anti-inflammatory and analgesic effects of the aqueous extract of corni fructus in murine RAW 264.7 macrophage cells," *Journal of Medicinal Food*, vol. 12, no. 4, pp. 788–795, 2009.

[14] W. H. Choi, J. P. Chu, M. H. Jiang, S. H. Baek, and H. D. Park, "Effects of fraction obtained from Korean Corni Fructus extracts causing anti-proliferation and p53-dependent apoptosis in A549 lung cancer cells," *Nutrition and Cancer*, vol. 63, no. 1, pp. 121–1292011, 2011.

[15] F. S. Hosseini, M. Noroozi Karimabad, M. R. Hajizadeh et al., "Evaluating of induction of apoptosis by Cornus mass L. extract in the gastric carcinoma cell line (AGS)," *Asian Pacific Journal of Cancer Prevention*, vol. 20, no. 1, pp. 123–130, 2019.

[16] H. Cai, G. Cao, and B. Cai, "Rapid simultaneous identification and determination of the multiple compounds in crudeFructus Corniand its processed products by HPLC-MS/MS with multiple reaction monitoring mode," *Pharmaceutical Biology*, vol. 51, no. 3, pp. 273–278, 2013.

[17] M. Radan, M. Dianat, M. Badavi, S. A. Mard, V. Bayati, and G. Goudarzi, "In vivo and in vitro evidence for the involvement of Nrf2-antioxidant response element signaling pathway in the inflammation and oxidative stress induced by particulate matter (PM10): the effective role of gallic acid," *Free Radical Research*, vol. 53, no. 2, pp. 210–225, 2019.

[18] M. Zhao, J. Tao, D. Qian et al., "Simultaneous determination of loganin, morroniside, catalpol and acteoside in normal and chronic kidney disease rat plasma by UPLC-MS for investigating the pharmacokinetics of Rehmannia glutinosa and Cornus officinalis Sieb drug pair extract," *Journal of Chromatography. B, Analytical Technologies in the Biomedical and Life Sciences*, vol. 1009, pp. 122–129, 2016.

[19] X. Gao, Y. Liu, L. Wang, N. Sai, Y. Liu, and J. Ni, "Morroniside inhibits H2O2-Induced podocyte apoptosis by down-regulating NOX4 expression controlled by autophagy in vitro," *Frontiers in Pharmacology*, vol. 11, article 533809, 2020.

[20] D. U. Kim, D. G. Kim, J. W. Choi et al., "Loganin attenuates the severity of acute kidney injury induced by cisplatin through the inhibition of ERK activation in mice," *International Journal of Molecular Sciences*, vol. 22, no. 3, p. 1421, 2021.

[21] Y. Yang, Y. Gu, H. Zhao, and S. Zhang, "Loganin attenuates osteoarthritis in rats by inhibiting IL-1β-Induced catabolism and apoptosis in chondrocytes via regulation of phosphatidylinositol 3-kinases (PI3K)/Akt," *Medical Science Monitor*, vol. 25, pp. 4159–4168, 2019.

[22] M. J. Kim, G. S. Bae, I. J. Jo et al., "Loganin protects against pancreatitis by inhibiting NF-κB activation," *European Journal of Pharmacology*, vol. 765, pp. 541–550, 2015.

[23] S. Liu, H. Shen, J. Li et al., "Loganin inhibits macrophage M1 polarization and modulates sirt1/NF-κB signaling pathway to attenuate ulcerative colitis," *Bopengimeered*, vol. 11, no. 1, pp. 628–639, 2020.

[24] M. Mihara and M. Uchiyama, "Determination of malonaldehyde precursor in tissues by thiobarbituric acid test," *Analytical Biochemistry*, vol. 86, no. 1, pp. 271–278, 1978.

[25] S. Komatsu, "Extraction of nuclear proteins," *Methods in Molecular Biology*, vol. 355, pp. 73–77, 2006.

[26] J. A. Lee, M. R. Shin, M. J. Kim, J. H. Lee, H. J. Park, and S. S. Roh, "Protective effects of inflammation of Curcumae Longae Rhizoma 30% EtOH extract on acute reflux esophagitis rats," *BioMed Research International*, vol. 2021, Article ID 8854945, 2021.

[27] J. Y. Kim, J. Leem, and H. L. Hong, "Protective effects of SPA0355, a thiourea analogue, against lipopolysaccharide-induced acute kidney injury in mice," *Antioxidant (Basel)*, vol. 9, no. 7, p. 585, 2020.

[28] Z. M. Zhang, L. Yang, Y. Wan et al., "The synergic renoprotective effect of Rehmanniae Radix Preparata and Corni Fructus on adenine-induced chronic kidney disease rats based on integrated plasma metabolomics and network pharmacology approach," *Life Sciences*, vol. 278, article 119545, 2021.

[29] Z. M. Zhang, L. Yang, Y. Wan et al., "Integrated gut microbiota and fecal metabolomics reveal the renoprotective effect of Rehmanniae Radix Preparata and Corni Fructus on adenine-induced CKD rats," *Journal of Chromatography. B, Analytical Technologies in the Biomedical and Life Sciences*, vol. 1174, article 122728, 2021.

[30] W. Ma, K. J. Wang, C. S. Cheng et al., "Bioactive compounds from _Cornus officinalis_ fruits and their effects on diabetic nephropathy," *Journal of Ethnopharmacology*, vol. 153, no. 3, pp. 840–845, 2014.

[31] K. Daenen, A. Andries, D. Mekahli, A. Van Schepdael, F. Jouret, and B. Bammens, "Oxidative stress in chronic kidney disease," *Pediatric Nephrology*, vol. 34, no. 6, pp. 975–991, 2019.

[32] S. R. Khan, "Stress oxidative: nephrolithiasis and chronic kidney diseases," *Minerva Medica*, vol. 104, no. 1, pp. 23–30, 2013.

[33] W. Manucha and P. G. Valles, "Apoptosis modulated by oxidative stress and inflammation during obstructive nephropathy," *Inflamm Allergy Drug Target*, vol. 11, no. 4, pp. 303–312, 2012.

[34] H. Esterbauer, P. Eckl, and A. Ortner, "Possible mutagens derived from lipids and lipid precursors," *Mutation Research*, vol. 238, no. 3, pp. 223–233, 1990.

[35] Y. Xu, J. Zhu, X. Hu et al., "CLIC1 inhibition attenuates vascular inflammation, oxidative stress, and endothelial injury," *PLoS One*, vol. 11, no. 11, article e0166790, 2016.

[36] L. Cheng, K. M. Harnett, W. Cao et al., "Hydrogen peroxide reduces lower esophageal sphincter tone in human esophagitis," *Gastroenterology*, vol. 129, no. 5, pp. 1675–1685, 2005.

[37] B. M. Babior, "NADPH oxidase," *Current Opinion in Immunology*, vol. 16, no. 1, pp. 42–47, 2004.

[38] E. Pick, "Using synthetic peptides for exploring protein-protein interactions in the assembly of the NADPH oxidase complex," *Methods in Molecular Biology*, vol. 1982, pp. 377–415, 2019.

[39] A. Djamali, A. Vidyasagar, G. Yagci, L. J. Huang, and S. Resese, "Mycophenolic acid may delay allograft fibrosis by inhibiting transforming growth factor-β1-induced activation of Nox-2 through the nuclear factor-κB pathway," *Transplantation*, vol. 90, no. 4, pp. 387–393, 2010.

[40] A. Djamali, A. Vidyasagar, M. Adulla, L. J. Huang, and S. Resese, "Nox-2 is a modulator of fibrogenesis in kidney allografts," *American Journal of Transplantation*, vol. 9, no. 1, pp. 74–82, 2009.

[41] S. M. Jeon, N. S. Chandel, and N. Hay, "AMPK regulates NADPH homeostasis to promote tumour cell survival during energy stress," *Nature*, vol. 485, no. 7400, pp. 661–665, 2012.

[42] S. M. Jeon, "Regulation and function of AMPK in physiology and diseases," *Experimental & Molecular Medicine*, vol. 48, no. 7, article e245, 2016.

[43] T. Bai, Y. Yang, Y. L. Yao et al., "Betulin alleviated ethanol-induced alcoholic liver injury via SIRT1/AMPK signaling pathway," *Pharmacological Research*, vol. 105, pp. 1–12, 2016.

[44] A. R. Parrish, "Matrix metalloproteinases in kidney disease: role in pathogenesis and potential as a therapeutic target," *Progress in Molecular Biology and Translational Science*, vol. 148, pp. 31–65, 2017.

[45] C. Bonnans, J. Chou, and Z. Werb, "Remodelling the extracellular matrix in development and disease," *Nature Reviews. Molecular Cell Biology*, vol. 15, no. 12, pp. 786–801, 2014.

[46] Q. Yuan, R. J. Tan, and Y. Liu, "Myofibroblast in kidney fibrosis: origin, activation, and regulation," *Advances in Experimental Medicine and Biology*, vol. 1165, pp. 253–283, 2019.

[47] X. M. Meng, P. M. K. Tang, J. Li, and H. Y. Lan, "TGF-Î²/Smad signaling in renal fibrosis," *Frontiers in Physiology*, vol. 6, p. 82, 2015.

[48] H. H. Hu, D. Q. Chen, Y. N. Wang et al., "New insights into TGF-β/Smad signaling in tissue fibrosis," *Chemico-Biological Interactions*, vol. 292, pp. 76–83, 2018.

[49] Y. Zhang, S. Wang, S. Liu, C. Li, and J. Wang, "Role of Smad signaling in kidney disease," *International Urology and Nephrology*, vol. 47, no. 12, pp. 1965–1975, 2015.